Hindawi Publishing Corporation
Advances in Civil Engineering
Volume 2011, Article ID 463638, 13 pages
doi:10.1155/2011/463638

Research Article

Chemical, Mineralogical, and Morphological Properties of Steel Slag

Irem Zeynep Yildirim[1] and Monica Prezzi[2]

[1] *Fugro Consultants, Inc., 6100 Hillcroft Avenue (77081), Houston, TX, 77274, USA*
[2] *School of Civil Engineering, Purdue University, 550 Stadium Mall Drive, West Lafayette, IN, 47907, USA*

Correspondence should be addressed to Irem Zeynep Yildirim, iremzeynep@gmail.com

Received 2 February 2011; Accepted 27 July 2011

Academic Editor: J. Antonio H. Carraro

Steel slag is a byproduct of the steelmaking and steel refining processes. This paper provides an overview of the different types of steel slag that are generated from basic-oxygen-furnace (BOF) steelmaking, electric-arc-furnace (EAF) steelmaking, and ladle-furnace steel refining processes. The mineralogical and morphological properties of BOF and electric-arc-furnace-ladle [EAF(L)] slag samples generated from two steel plants in Indiana were determined through X-Ray Diffraction (XRD) analyses and Scanning Electron Microscopy (SEM) studies. The XRD patterns of both BOF and EAF(L) slag samples were very complex, with several overlapping peaks resulting from the many minerals present in these samples. The XRD analyses indicated the presence of free MgO and CaO in both the BOF and EAF(L) slag samples. SEM micrographs showed that the majority of the sand-size steel slag particles had subangular to angular shapes. Very rough surface textures with distinct crystal structures were observed on the sand-size particles of BOF and EAF(L) slag samples under SEM. The characteristics of the steel slag samples considered in this study are discussed in the context of a detailed review of steel slag properties.

1. Introduction

The steelmaking industries in the US generate 10–15 million tons of steel slag every year. Approximately 15 to 40% of the steel slag output is initially stockpiled in the steel plants and, eventually, sent to slag disposal sites. Utilization of steel slag in civil engineering applications can alleviate the need for their disposal and reduce the use of natural resources. A better understanding of the properties of steel slag is required for large volumes of this material to be utilized in a technically sound manner in civil engineering applications.

Knowledge of the chemical, mineralogical, and morphological properties of steel slags is essential because their cementitious and mechanical properties, which play a key role in their utilization, are closely linked to these properties. As an example, the frictional properties of steel slag are influenced by its morphology and mineralogy. Similarly, the volumetric stability of steel slag is a function of its chemistry and mineralogy. The chemical, mineralogical, and morphological characteristics of steel slag are determined by the processes that generate this material. Therefore, knowledge of the different types of steelmaking and refining operations that produce steel slag as a byproduct is also required. This paper provides an overview of steel slag generation and a literature review on the chemical and mineralogical properties of steel slags. Moreover, the mineralogical and morphological characteristics of steel slag samples generated from two steel plants in Indiana were evaluated through XRD analyses and SEM studies.

2. Overview

Slags are named based on the furnaces from which they are generated. Figure 1 shows a flow chart for the iron and steelmaking processes and the types of slag generated from each process [1, 2].

The main types of slags that are generated from the iron and steelmaking industries are classified as follow:

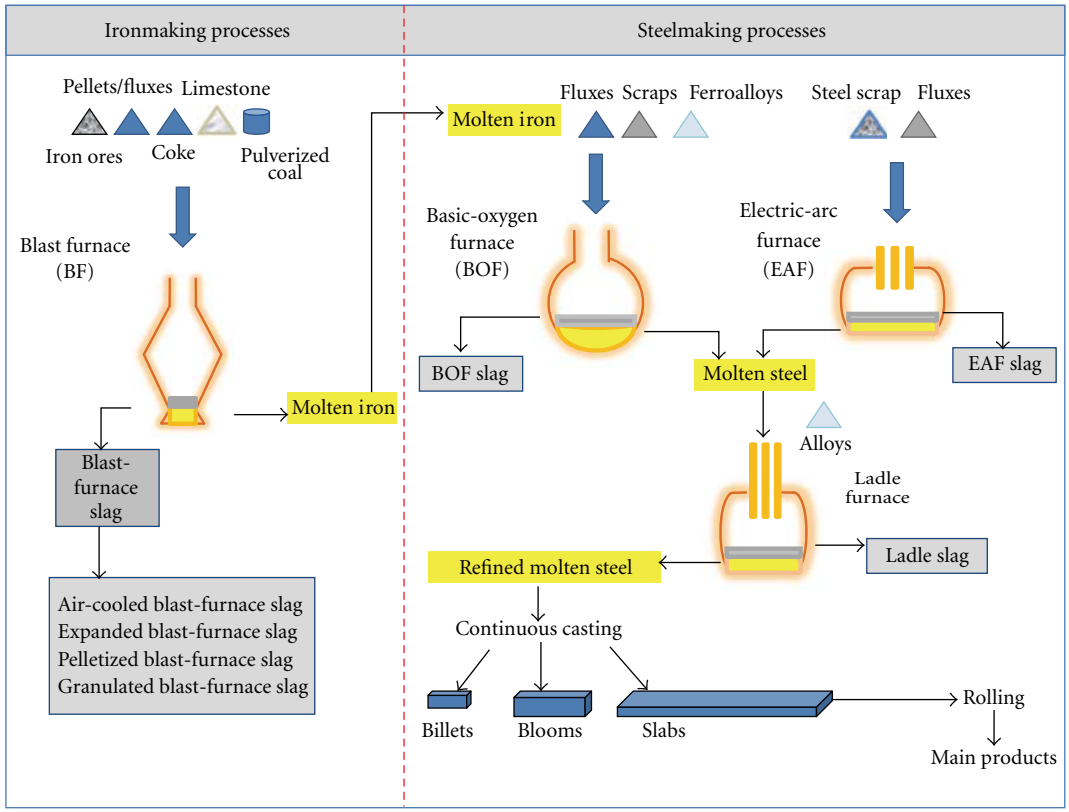

Figure 1: Flowchart of iron and steelmaking processes [1, 2].

(i) blast-furnace slag (ironmaking slag),

(ii) steel-furnace slag,

(a) basic-oxygen-furnace (BOF) slag,

(b) electric-arc-furnace (EAF) slag,

(c) ladle slag.

2.1. Basic-Oxygen-Furnace Process of Steelmaking and Slag Generation. Basic-oxygen furnaces, which are located at integrated steel mills in association with a blast furnace, are charged with the molten iron produced in the blast furnace and steel scraps. Typically, the proper basic-oxygen furnace charge consists of approximately 10–20% of steel scrap and 80–90% of molten iron [1, 3]. The presence of steel scraps in the basic-oxygen furnace charge plays an important role in cooling down the furnace and maintaining the temperature at approximately 1600°C–1650°C for the required chemical reactions to take place.

Figure 2 shows a schematic representation of a basic-oxygen furnace [1, 4]. First, steel scrap is charged to the furnace and, immediately after this charge, a ladle of molten iron (~200 tons) is poured on top of it with the help of a crane. Then an oxygen lance, lowered into the furnace, blows 99% pure oxygen on the charge at supersonic speeds. During the blowing cycle, which lasts approximately 20–25 minutes, intense oxidation reactions remove the impurities of the charge. Carbon dissolved in the steel is burned to form carbon monoxide, causing the temperature to rise to 1600–1700°C (the temperature in the furnace is carefully monitored throughout the oxygen blowing period). The scrap is thereby melted, and the carbon content of the molten iron

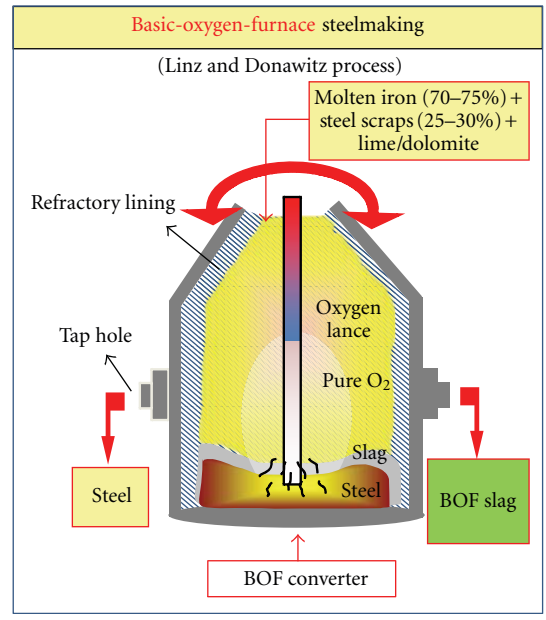

Figure 2: Schematic representation of the basic-oxygen furnace process [1, 4].

is lowered [1, 3]. In order to remove the unwanted chemical elements of the melt, the furnace is also charged with fluxing agents, such as lime (CaO) or dolomite ($MgCa(CO_3)_2$), during the oxygen blowing cycles. The impurities combine with the burnt lime or dolomite forming slag and reducing the amount of undesirable substances in the melt. Samples of the molten metal are collected near the end of the blowing cycle and tested for their chemical composition. Once the desired chemical composition is achieved, the oxygen lance is pulled up from the furnace.

Slag resulting from the steelmaking process floats on top of the molten steel. The basic-oxygen furnace is tilted in one direction in order to tap the steel into ladles. The steel produced in the basic-oxygen furnace can either undergo further refining in a secondary refining unit or be sent directly to a continuous caster where semifinished shapes (blooms, billets, or slabs) are solidified in integrated steel mills. After all the steel is removed from the basic-oxygen furnace, it is tilted again in the opposite direction to pour the liquid slag into ladles. The slag generated from a steelmaking cycle is later processed, and the final product after processing is referred to as *basic-oxygen-furnace slag* (BOF slag). The chemical reactions occurring during the removal of impurities determine the chemical composition of the basic-oxygen-furnace slag [1, 3, 5].

2.2. Electric-Arc-Furnace (EAF) Process of Steelmaking and Slag Generation. Electric-arc furnaces (mini mills) use high-power electric arcs, instead of gaseous fuels, to produce the heat necessary to melt recycled steel scrap and to convert it into high quality steel. The electric-arc furnace steelmaking process is not dependent on the production from a blast furnace since the main feed for it is steel scrap with some pig iron. Electric-arc furnaces are equipped with graphite electrodes and resemble giant kettles with a spout or an eccentric notch on one side. The roof of the electric-arc furnaces can pivot and swing to facilitate the loading of raw materials. Steel scraps, either as heavy melt (large slabs and beams) or in shredded form are separated, graded, and sorted into different classes of steel in scrap yards. Scrap baskets are loaded carefully with different types of scrap according to their size and density to ensure that both the melting conditions in the furnace and the chemistry of the finished steel are within the targeted range [1–3].

The electric-arc furnace steelmaking process starts with the charging of various types of steel scrap to the furnace using steel scrap baskets. Next, graphite electrodes are lowered into the furnace. Then, an arc is struck, which causes electricity to travel through the electrodes and the metal itself. The electric arc and the resistance of the metal to this flow of electricity generate the heat. As the scrap melts, the electrodes are driven deeper through the layers of scrap. In some steel plants, during this process, oxygen is also injected through a lance to cut the scrap into smaller sizes. As the melting process progresses, a pool of liquid steel is generated at the bottom of the furnace. CaO, in the form of burnt lime or dolomite, is either introduced to the furnace together with the scrap or is blown into the furnace during melting. After several baskets of scraps have melted, the refining metallurgical operations (e.g., decarburization and dephosphorization) are performed. During the steel refining period, oxygen is injected into the molten steel through an oxygen lance. Some iron, together with other impurities in the hot metal, including aluminum, silicon, manganese, phosphorus, and carbon, are oxidized during the oxygen injections. These oxidized components combine with lime (CaO) to form slag. As the steel is refined, carbon powder is also injected through the slag phase floating on the surface of the molten steel, leading to the formation of carbon monoxide. The carbon monoxide gas formed causes the slag to foam, thereby increasing the efficiency of the thermal energy transfer. Once the desired chemical composition of the steel is achieved, the electric-arc furnace is tilted, and the slag and steel are tapped out of the furnace into separate ladles. Steel is poured into a ladle and transferred to a secondary steelmaking station for further refining. The molten slag is carried to a slag-processing unit with ladles or slag pot carriers [1–3, 5].

In electric-arc furnaces, up to 300 tons of steel can be manufactured per cycle (a cycle takes one to three hours to complete). Initially, the EAF steelmaking process was more expensive than the BOF process and, hence, it was only used for production of high quality steels. However, as the size of the electric-arc furnaces increased over the years, the EAF steelmaking process has become competitive in the production of different grades of steel and has started to dominate the US steel industry with a 55% share of the total steel output in 2006, according to USGS [6].

2.3. Ladle Furnace Refining and Slag Generation. After completion of the primary steelmaking operations, steel produced by the BOF or EAF processes can be further refined to obtain the desired chemical composition. These refining processes are called secondary steelmaking operations. Refining processes are common in the production of high-grade steels. The most important functions of secondary refining processes are final desulfurization, degassing of oxygen, nitrogen, and hydrogen, removal of impurities, and final decarburization (done for ultralow carbon steels). Depending on the quality of the desired steel, molten steel produced in the EAF and BOF process goes through some or all of the above mentioned refining processes [1, 2]. Most of the mini mills and integrated steel mills have ladle-furnace refining stations for secondary metallurgical processes. Figure 3 shows a schematic representation of an electric-arc-furnace and a ladle-refining unit associated with it [2, 4].

Ladle furnaces, which look like smaller versions of EAF furnaces, also have three graphite electrodes connected to an arc transformer used to heat the steel. Typically, the bottom of the ladle furnace has a pipeline through which argon gas is injected for stirring and homogenization of the liquid steel in the furnace. By injecting desulfurizing agents (such as Ca, Mg, CaSi, CaC_2) through a lance, the sulfur concentration in the steel can be lowered to 0.0002% [1]. The addition of silicon and aluminum during deoxidation forms silica (SiO_2) and alumina (Al_2O_3); these oxides are later absorbed by the slag generated by the refining process. In addition,

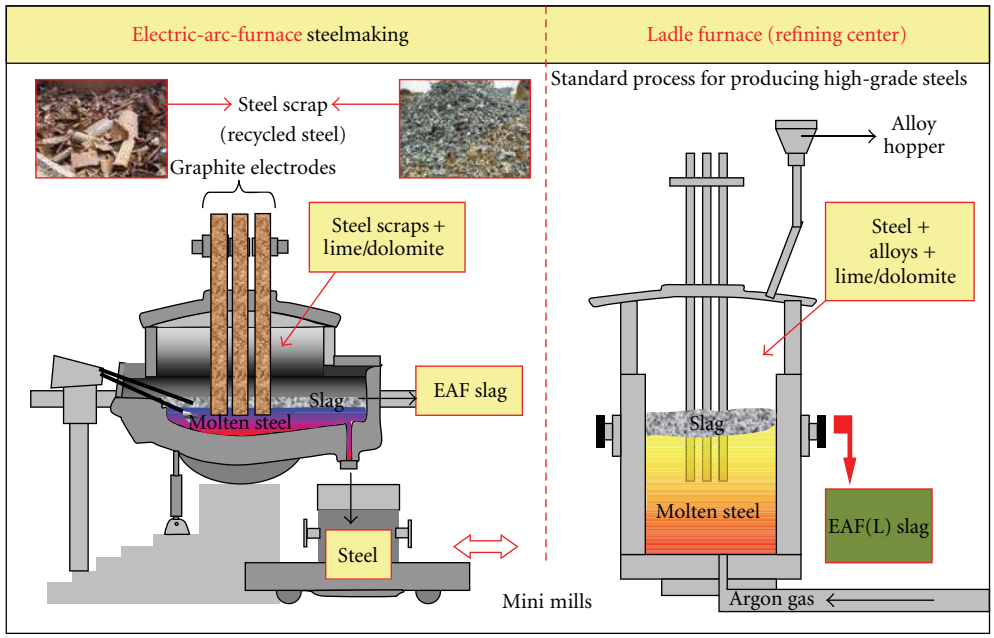

Figure 3: Schematic representation of the electric-arc-furnace steelmaking and ladle refining process [2, 4].

in order to adjust precisely the chemical composition of the steel to produce different grades of steel, the desired alloys are added to the molten steel through an alloy hopper that is connected to the ladle furnace. Ladle furnaces also function as a storage unit for the steel before the initiation of casting operations. Therefore, ladle furnaces reduce the cost of high-grade steel production and allow flexibility in the steelmaking operations [1, 2].

3. Chemical Composition of Steel Slags

Both BOF and EAF slags are formed during basic steelmaking operations, as explained above. Therefore, in general, the chemical and mineralogical compositions of BOF and EAF slags are similar. Calcium oxide and iron oxide are the two major chemical constituents of both EAF and BOF slags. Ladle slag is generated during the steel refining processes in which several alloys are added to the ladle furnace to produce different grades of steel. For this reason, the chemical constituents of ladle slag differ from those of BOF and EAF slags. Table 1 provides the chemical composition of basic-oxygen-furnace (BOF), electric-arc-furnace (EAF), and ladle slags from various sources [7–22].

The main chemical constituents of the basic-oxygen-furnace slag are CaO, FeO, and SiO_2. During the conversion of molten iron into steel, a percentage of the iron (Fe) in the hot metal cannot be recovered into the steel produced. This oxidized iron is observed in the chemical composition of the BOF slag. Depending on the efficiency of the furnace, the iron oxide (FeO/Fe_2O_3) content of BOF slag can be as high as 38% (refer to Table 1); this is the amount of oxidized iron that cannot be recovered during the conversion of molten iron into steel. The silica (SiO_2) content of BOF slag ranges from 7 to 18%. The Al_2O_3 and MgO contents are in the 0.5–4% and 0.4–14% ranges, respectively. The free lime content can be as high as 12%. Large quantities of lime or dolomotic lime are used during the process of conversion from iron to steel and, hence, the CaO content of BOF slag is typically very high (CaO >35%) [1, 8, 12, 23].

EAF slag has a chemical composition similar to that of BOF slag (refer to Table 1). The EAF steelmaking process is essentially a steel scrap recycling process. Therefore, the chemical composition of EAF slag depends significantly on the properties of the recycled steel. Compared to BOF slags, the main chemical constituents of EAF slags can vary widely. Typically, the FeO, CaO, SiO_2, Al_2O_3, and MgO contents of EAF slags are in the 10–40%, 22–60%, 6–34%, 3–14%, and 3–13% ranges, respectively. Other minor components include other oxidized impurities, such as MgO, MnO, and SO_3. EAF slags also contain free CaO and MgO along with other complex minerals and solid solutions of CaO, FeO, and MgO. The FeO content of EAF slags generated from stainless steel production processes can be as low as 2% [24].

Information on the chemical composition of ladle slags (LS) is limited in the literature. During the steel refining process, different alloys are fed into the ladle furnace in order to obtain the desired steel grade. Hence, the chemical composition of ladle slag is highly dependent on the grade of steel produced. As a result, compared to BOF and EAF slags, the chemical composition of ladle slag is highly variable. Typically, the FeO content of ladle slag is much lower (<10%) than that of EAF and BOF slags. On the other hand, the Al_2O_3 and CaO contents are typically higher for ladle slags (refer to Table 1).

Table 1: Chemical composition of BOF, EAF, and Ladle Slags.

		Oxide composition (%)											
Reference	Slag type	CaO	SiO_2	Al_2O_3	MgO	FeO	Fe_2O_3	Fe_{total}	SO_3	MnO	TiO_2	P_2O_5	Free CaO
Das et al. [7]	BOF	47.9	12.2	1.2	0.8	26.3	—	—	0.3	0.3	—	3.3	—
Juckes [8][a]	BOF	36.4–45.8	10.7–15.2	1–3.4	4.1–7.8	—	—	19–24	0.1–0.2	2.7–4.3	—	1–1.5	2.5–12
Mahieux et al. [9]	BOF	47.5	11.8	2.0	6.3	—	22.6	—	—	1.9	0.5	2.7	—
Poh et al. [10]	BOF	52.2	10.8	1.3	5.04	17.2	10.1	—	—	2.5	0.6	1.3	10.2
Shen et al. [11]	BOF	39.3	7.8	0.98	8.56	—	38.06	—	0.0	4.2	0.9	—	—
Shi [12]	BOF	30–55	8–20	1–6	5–15	10–35	—	—	0.1–0.2	2–8	0.4–2	0.2–2	—
Tossavainen et al. [13]	BOF	45.0	11.1	1.9	9.6	10.7	10.9	—	—	3.1	—	—	—
Waligora et al. [14]	BOF	47.7	13.3	3.0	6.4	—	24.4			2.6	0.7	1.5	9.2
Xuequan et al. [15][b]	BOF	45–60	10–15	1–5	3–13	7–20	3–9	—	—	—	—	1–4	—
Barra et al. [16]	EAF	29.5	16.1	7.6	5.0	—	32.56	—	0.6	4.5	0.78	0.6	—
Luxán et al. [17]	EAF	24.4	15.4	12.2	2.9	34.4	—	—	—	5.6	0.56	1.2	—
Manso et al. [18]	EAF	23.9	15.3	7.4	5.1	—	—	42.5	0.1	4.5	—	—	0.5
Shi [12]	EAF	35–60	9–20	2–9	5–15	15–30	—	—	0.1–0.2	3–8	—	0.0–0.3	—
Tossavainen et al. [13]	EAF	38.8	14.1	6.7	3.9	5.6	20.3	—	—	5	—	—	—
Tsakiridis et al. [19]	EAF	35.7	17.5	6.3	6.5	—	26.4	—	—	2.5	0.8	—	—
Nicolae et al. [20]	Ladle	49.6	14.7	25.6	7.9	0.44	0.22	0.17	0.8	0.4	—	0.2	—
Shi [12]	Ladle	30–60	2–35	5–35	1–10	0–15	—	—	0.1–1	0–5.0	—	0.1–0.4	—
Qian et al. [21]	Ladle	49.5	19.59	12.3	7.4	—	0.9	—	—	1.4	—	0.4	2.5
Setién et al. [22]	Ladle	50.5–57.5	12.6–19.8	4.3–18.6	7.5–11.9	—	1.6–3.3	—		0.4–0.5	0.3–0.9	0–0.01	3.5–19
Tossavainen et al. [13]	Ladle	42.5	14.2	22.9	12.6	0.5	1.1	0.4	—	0.2	—	—	—

[a] The range of values are compiled based on the chemical composition data from 4 different sources in Great Britain provided by Juckes [8].
[b] Xuequan et al. [15] report chemical composition of steel slag from refining process (not specified as BOF).
— = data not available.

4. Mineralogical Properties of Steel Slag

Crystal formation is a function of both the chemical composition of the melt and its cooling rate. Silica rich blast-furnace slag vitrifies (forms a glassy phase) easily when it is rapidly cooled. Steel slag has a lower silica content than blast-furnace slag and, hence, steel slag seldom vitrifies even when rapidly cooled. Tossavainen et al. [13] studied the effect of the cooling rate on the mineralogy of BOF, EAF, and ladle slag samples with different proportions of major chemical constituents and showed that ladle slag rapidly cooled using the water granulation technique becomes almost completely amorphous, with the exception of the crystalline phase of periclase (MgO). On the other hand, the rapidly cooled (granulated) BOF and EAF slag samples showed very complex crystalline structures similar to those of slowly cooled BOF and EAF slag samples. Reddy et al. [25] also identified a very crystalline structure in quenched BOF slag using XRD analysis. These studies indicate that even when rapidly cooled, in general, steel slag tends to crystallize due to its chemical composition.

Several researchers studied the mineralogical composition of steel slags. X-ray diffraction analysis of steel slag samples shows a complex structure with many overlapping peaks reflecting the crystalline phases present in steel slag. These crystalline phases appear to be mainly due to the chemical composition of steel slag and the slow cooling rate applied during processing [1, 26–28]. The feed (charge) into the furnaces vary from one steelmaking plant to another, so variations in the chemical constituents of steel slags produced at different steelmaking plants are expected. A variety of mineral phases were identified and reported in the literature for EAF, BOF, and ladle slags. Table 2 presents the minerals identified in steel slags, as reported in the literature [8, 13, 16, 17, 20, 21, 25, 28–30].

The common mineral phases present in steel slags include merwinite ($3CaO{\cdot}MgO{\cdot}2SiO_2$), olivine ($2MgO{\cdot}2FeO{\cdot}SiO_2$), β-C_2S ($2CaO{\cdot}SiO_2$), α-C_2S, C_4AF ($4CaO{\cdot}Al_2O_3{\cdot}FeO_3$), C_2F ($2CaO{\cdot}Fe_2O_3$), CaO (free lime), MgO, FeO and C_3S ($3CaO{\cdot}SiO_2$), and the RO phase (a solid solution of CaO-FeO-MnO-MgO) [21, 24, 31], as can be seen in Table 2. Since BOF and EAF slags both have high iron oxide contents, solid solutions of FeO (wustite) are typically observed as one of the main mineral phases. Ladle slag has a lower FeO content, and polymorphs of C_2S are therefore frequently observed as the main phase [19, 24, 27, 29].

Due to the presence of unstable phases in its mineralogy, steel slags can show volumetric instability, caused mainly by the presence of free CaO. In the presence of water, free lime hydrates and forms portlandite ($Ca(OH)_2$). Portlandite has a lower density than CaO and, hence, hydration of free CaO results in volume increase. Ramachandran et al. [32] studied the hydration mechanism of CaO and proved that when it is immersed in water, compacted CaO can hydrate almost completely in a few days with a volume increase as high as 100%. Their study also demonstrated that hydration of lime by exposure to water vapor causes more expansion than hydration caused by exposure to water due to the effect of temperature. The fact that limes hydrates quickly suggests that the majority of the free lime in steel slag will hydrate in a few days if it is given access to water. However, residual lime can be embedded in small pockets in gravel-size steel slag particles. Figure 4 depicts a gravel-size BOF slag particle with a lime pocket (seen in white). Lime pockets may not hydrate at all if they are not given access to water through the fractures extending to them. If there are fractures in the slag particles extending to these lime pockets, then hydration can progress [8, 12, 33].

Figure 4: Gravel-size steel slag particle with a lime pocket (photograph taken at Mittal Steel, Indiana Harbor West Plant).

Other expansive compounds, such as free MgO, may also be present in steel slag. Unlike CaO, free MgO hydrates at a much slower rate, causing significant volume changes for months or even years. In general, slags generated from modern steelmaking technologies have low MgO content. However, if dolomite ($CaMg(CO_3)_2$) is used as a fluxing agent instead of lime, the free MgO content in steel slag increases and, therefore, the possibility of volumetric expansion due to hydration of MgO increases as well [8, 34–37].

Another reaction that causes volumetric expansion involves the dicalcium silicate (C_2S) phase. The C_2S phase is commonly present in all types of steel slags and, in particular, is abundant typically as the main phase in ladle slags. C_2S exists in four well-defined polymorphs: α, α', β, and γ. α-C_2S is stable at high temperatures (>630°C). At temperatures below 500°C, β-C_2S starts transforming into γ-C_2S. This transformation produces volumetric expansion of up to 10%. If the steel slag cooling process is slow, crystals break, resulting in a significant amount of dust. This phase conversion and the associated dusting are typical for ladle slags. For this reason, ladle slags are commonly called "self-dusting" or "falling" slags [8, 27].

5. Characterization of Steel Slag from Indiana Steel Plants

5.1. Materials. The chemical composition, mineralogy, and morphology of steel slag particles can influence both the cementitious characteristics and mechanical properties of steel slag. Two different types of steel slag (BOF and EAF ladle slags) generated from Indiana steel plants were considered in this study.

Table 2: Mineralogical phases of BOF, EAF, and ladle slags.

Reference	Slag	Mineralogical phases
Barra et al. [16]	EAF	$CaCO_3$, FeO, MgO, Fe_2O_3, $Ca_2Al(AlSiO_7)$, Ca_2SiO_4
Geiseler [29]	—	$2CaO\cdot SiO_2$, $3CaO\cdot SiO_2$, $2CaO\cdot Fe_2O_3$, FeO, (Ca, Fe)O (calciowustite), (Mg, Fe)O (magnesiowustite), free MgO, CaO
Juckes [8]	BOF	C_3S, C_2S, C_2F, RO phase (FeO-MgO-CaO-FeO), MgO, CaO
Luxán et al. [17]	EAF	Ca_2SiO_5, $Ca_2Al(AlSiO_7)$, Fe_2O_3, $Ca_{14}Mg_2(SiO_4)_8$, $MgFe_2O_4$, Mn_3O_4, MnO_2
Manso et al. [28]	Ladle	Al_2O_4Mg, $Ca(OH)_2$, Si_2O_6CaMg, MgO, Ca_3SiO_5, β-Ca_2SiO_4, γ-Ca_2SiO_4, SO_4Ca
Nicolae et al. [20]	BOF	$2CaO\cdot Al_2O_3\cdot SiO_2$, Fe_2O_3, CaO, FeO
Nicolae et al. [20]	EAF	MnO_2, MnO, Fe_2SiO_4, Fe_7SiO_{10}
Nicolae et al. [20]	Ladle	$CaO\cdot SiO_2$, $CaOAl_2O_3\cdot 2SiO_2$, CaS, Al_2O_3
Qian et al. [21]	EAF	γ-Ca_2SiO_4, C_3MS_2, CFMS, FeO-MnO-MgO solid solution
Qian et al. [21]	Ladle	γ-Ca_2SiO_4, C_3MS_2, MgO
Reddy et al. [25]	BOF	$2CaO\cdot Fe_2O_3$, $2CaO\cdot P_2O_5$, $2CaO\cdot SiO_2$, CaO
Reddy et al. [25]	BOF[q]	$2CaO\cdot Fe_2O_3$, $3CaO\cdot SiO_2$, $2CaO\cdot SiO_2$, Fe_2O_3
Tossavainen et al. [13]	Ladle	$Ca_{12}Al_{14}O_{33}$, $MgO\cdot\beta$-Ca_2SiO_4, γ-Ca_2SiO_4, $Ca_2Al_2SiO_7$
Tossavainen et al. [13]	BOF	β-Ca_2SiO_4, FeO-MnO-MgO solid solution, MgO
Tossavainen et al. [13]	EAF	$Ca_3Mg(SiO_4)_2$, β-Ca_2SiO_4, Spinel solid solution (Mg, Mn)(Cr, Al)$_2O_4$, wustite-type solid solution ((Fe, Mg, Mn)O), $Ca_2(Al, Fe)_2O_5$
Tsakiridis et al. [19]	EAF	Ca_2SiO_4, $4CaO\cdot Al_2O_3\cdot Fe_2O_3$, $Ca_2Al(AlSiO_7)$, Ca_3SiO_5, $2CaO\cdot Al_2O_3\cdot SiO_2$, FeO, Fe_3O_4, MgO, SiO_2
Wachsmuth et al. [30]	BOF	Ca_2SiO_4, Ca_3SiO_5, FeO, $2CaO\cdot Fe_2O_3$

[q] quenched; — = type of slag not provided.

Mittal Steel, Indiana Harbor Works West Plant, which is located in Highland, Indiana, was the source plant for the BOF slag. Multiserv Ltd., Harsco Corporation, which performs slag processing operations at the Mittal Steel Plant, supplied representative samples of BOF slag consisting of particles smaller than 15 mm. The Whitesville Steel Mill at Nucor Steel, which is located in Crawfordsville, Indiana, was the source for the EAF ladle (L) slag. The Edward C. Levy Co., which operates at the Whitesville Steel Mill, supplied The EAF(L) slag. This slag is referred to as EAF(L) slag, as it is the ladle slag generated from the refining of the steel from the electric-arc furnace. Edward C. Levy Co. provided representative samples of EAF(L) slag consisting of particles smaller than 9.5 mm.

5.2. Testing Methods. The oxide composition of both the BOF slag and EAF(L) samples was determined by the slag processing companies (Multiserv and Edward C. Levy Co.) using X-ray fluorescence (XRF) analysis. In order to determine the mineralogical phases present in the steel slag samples, X-ray diffraction analyses were carried out on both BOF slag and on EAF(L) slag samples with a Siemens D-500 diffractometer using copper radiation. Representative oven-dried steel slag samples (with both gravel-size and finer particles) were crushed until a powder passing the No. 200 (0.075 mm opening) sieve was attained. The powder samples were step-scanned from 5 to 65° (2θ) in 0.02° increments and 1 s count time. The X-ray diffraction patterns of the steel slag samples were analyzed by comparing the peaks present in the XRD patterns with those provided in The Joint Committee for Powder Diffraction Standards, Hanawalt System for identification of inorganic compounds (JCPDS). The software program Jade was also used to help identify the minerals present in the samples. Only qualitative analyses were performed due to the presence of overlapping peaks in the XRD patterns and to the complexity of the crystalline phases in the slag samples tested. The main, minor, and probable phases were determined for each slag sample tested.

Table 3: Chemical composition of BOF slag.

Oxides	% (by weight)
CaO	39.40
FeO	30.23
SiO_2	11.97
MgO	9.69
MnO	2.74
Al_2O_3	2.16
P_2O_5	1.00
TiO_2	0.40
Na_2O	0.25
Cr_2O_3	0.20
K_2O	0.05
Cl	0.01
SO_3	0.12
L.O.I.[a]	1.80

[a] L.O.I: Loss on ignition.

Table 4: Mineralogical phases identified in BOF slag based on XRD analyses.

Mineral type	Formula	BOF slag
Portlandite	$Ca(OH)_2$	major
Srebrodol'skite	$Ca_2Fe_2O_5$	major
Merwinite	$Ca_3Mg(SiO_4)_2$	major
Larnite	Ca_2SiO_4	minor
Calcite (manganoan)	$(Ca, Mn)CO_3$	minor
Lime	CaO	minor
Dolomite	$CaMg(CO_3)_2$	minor
Wollastonite	$CaSiO_3$	probable
Periclase	MgO	probable
Pentahydrite	$MgSO_4 \cdot 5H_2O$	probable
Monticellite	$CaMgSiO_4$	probable
Hematite	Fe_2O_3	probable
Magnesite	$MgCO_3$	probable

Table 5: Chemical composition of EAF(L) slag.

Oxides	% (by weight)
CaO	47.52
Al_2O_3	22.59
FeO	7.61
MgO	7.35
SiO_2	4.64
SO_3	2.28
MnO	1.00
Cr_2O_3	0.37
TiO_2	0.33
P_2O_5	0.09
Na_2O	0.06
K_2O	0.02
Zn	0.01
L.O.I[a]	6.20

[a] L.O.I: Loss on ignition.

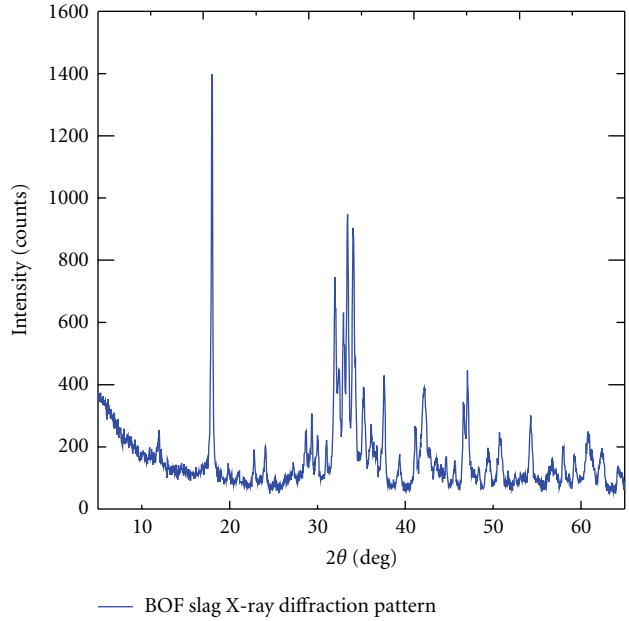

Figure 5: X-ray diffraction pattern for BOF slag.

Figure 6: Gravel-size BOF slag particles.

Steel slag particles were subjected to microscopic examination to characterize their shape, angularity, and surface texture. The examination was performed with a scanning electron microscope (manufactured by ASPEX, Model Personal SEM) and a light microscope (manufactured by Nikon). The shape and surface texture of the gravel-size particles were visible to the naked eye. The medium sand-size particles were examined under the light microscope. Finer sand and silt-size particles were examined under the SEM. To prevent charging of the steel slag particles, they were coated with palladium with the Hummer 6.2 sputtering system. The coated steel slag particles were examined on a two-sided copper tape. The SEM images were captured on both photomicrographs and digital files.

6. Chemical Composition and Particle Mineralogy of BOF Slag

Table 3 gives the oxide composition of the BOF slag samples. The percentages of most of the oxides present in the BOF slag samples tested in this study are within the ranges reported by other researchers [8, 10, 13, 38, 39]. However, the FeO content of the tested BOF slag samples is slightly higher than that of most of the BOF slags reported in the literature.

The XRD patterns of the BOF slag samples were very complex, with several overlapping peaks resulting from the many minerals present in the samples (see Figure 5). BOF slag is cooled slowly in slag pits thereby allowing enough time for formation of well-defined crystals. Several other researchers have reported similar, complex XRD patterns for BOF slag [13, 20, 25].

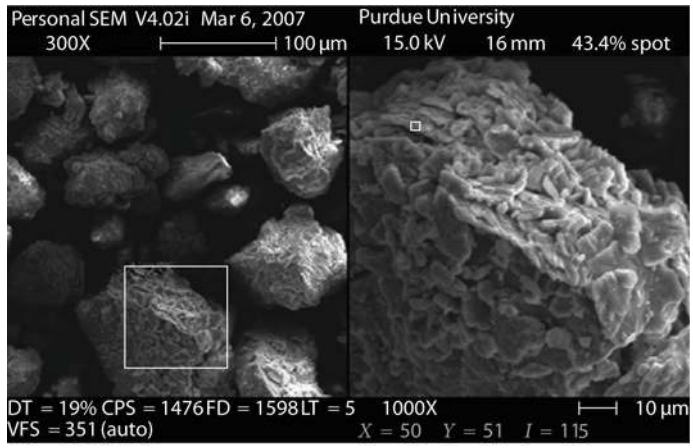

(a)

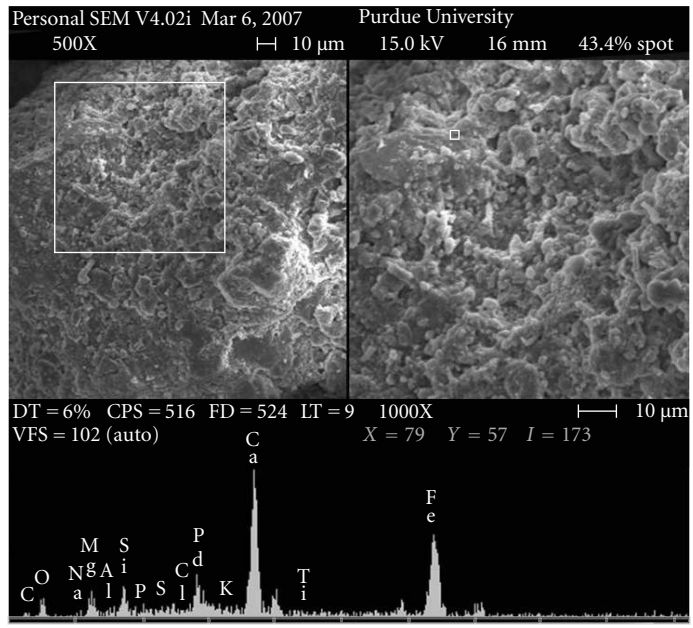

(b)

Figure 7: SEM micrographs of BOF slag sample. (a) Particle shape and (b) surface texture and elemental analysis.

Table 4 summarizes all of the mineral phases that were identified in the BOF slag samples. The mineral phases identified in the BOF slag samples were determined as major or minor phases depending on the intensity of the peaks, which is an indication of the quantity of the minerals present in the samples. It is important to note that the very complex mineralogical composition of BOF slag, with many overlapping peaks and different solid solutions of oxides (FeO and MgO), makes the identification of the phases very difficult. Therefore, some of the overlapping mineral phases that could not be determined with certainty were identified as probable. The most abundant mineral phase present in BOF slag is portlandite ($Ca(OH)_2$). The presence of this mineral is expected since BOF slag contains 39% lime (CaO), which in the presence of moisture, converts to $Ca(OH)_2$. The other major phases included merwinite ($Ca_3Mg(SiO_4)_2$), and srebrodol'skite ($Ca_2Fe_2O_5$). The presence of free lime (CaO) and the probable presence of free magnesia (MgO) in the samples are an indication of the potential for volumetric instability of the tested BOF slag.

7. BOF Slag Particle Morphology

Figure 6 shows the gravel-size particles of BOF slag. The gravel-size particles of BOF slag had shapes varying from subrounded to subangular. Distinct asperities and edges were visible in subangular, bulky particles. Most of the gravel-size particles had a high sphericity and a solid structure. A heterogeneous porous structure was also observed on the surface of a few particles.

Figures 7(a) and 7(b) are SEM micrographs showing the shape and surface texture of BOF slag particles, respectively. The SEM studies showed that the sand- and silt-size BOF slag

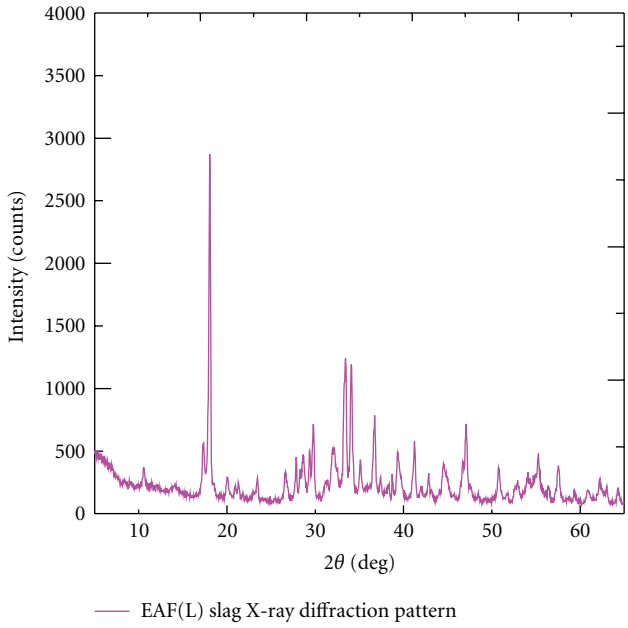

Figure 8: X-ray diffraction patterns for EAF(L) slag.

Figure 9: Gravel-size EAF(L) slag particles.

Table 6: Mineralogical phases identified in EAF(L) slag based on XRD analyses.

Mineral type	Formula	EAF(L) slag
Portlandite	$Ca(OH)_2$	major
Mayenite	$Ca_{12}Al_{14}O_{33}$	major
Larnite	Ca_2SiO_4	minor
Lime	CaO	minor
Uvavorite	$Ca_3 \cdot Cr_2(SiO_4)_3$	minor
Wollastonite[f]	$(Ca, Fe)SiO_3$	minor
Periclase	MgO	minor
Calcite	$CaCO_3$	probable
Merwinite	$Ca_3Mg(SiO_4)_2$	probable

[f] ferroan.

particles had subrounded to angular shapes. Distinct asperities and edges were visible in angular, bulky particles. Most of the sand- and silt-size particles examined under the SEM had rough surface textures.

8. Chemical Composition and Particle Mineralogy of EAF(L) Slag

Table 5 shows the oxide composition of the tested EAF(L) slag sample.

Shi [12] reported that the CaO, SiO_2, Al_2O_3, MgO, and FeO contents of ladle slag are in the ranges of 30–60%, 2–35%, 5–35%, 1–10%, and 0.1–15%, respectively. The SiO_2 content of the EAF(L) slag used in this study was slightly higher than the lower limit of the range reported by Shi [12]. The EAF(L) slag used in this research is cooled very slowly in the pits under ambient atmospheric conditions. These slow cooling conditions allow the formation of various crystalline phases; these are reflected in the very complex XRD patterns shown in Figure 8. Mineral phases with distinct peaks of high intensities and some overlapping peaks of low intensities were detected. Several other researchers have reported similar XRD patterns for EAF(L) slag [13, 20, 28].

Table 6 summarizes all the mineral phases that were identified in the EAF(L) slag samples. As done for BOF slag, the mineral phases identified in the EAF(L) slag samples were determined as major or minor depending on the intensity of the peaks. Some of the overlapping mineral phases that could not be determined with certainty were identified as probable. The two major mineral phases present in the EAF(L) slag samples were portlandite ($Ca(OH_2)$) and mayenite ($Ca_{12}Al_{14}O_{33}$). The highest peak in the XRD pattern of the EAF(L) slag samples was observed for portlandite (see Table 5). Other minor phases identified were lime (CaO), larnite (Ca_2SiO_4), uvavorite ($Ca_3 \cdot Cr_2(SiO_4)_3$), wollastonite $(Ca, Fe)SiO_3$), and periclase (MgO).

9. EAF(L) Slag Particle Morphology

Figure 9 shows the gravel-size particles of EAF(L) slag. The gravel-size particles of the EAF(L) slag sample had shapes varying from subrounded to subangular. Both bulky and platy gravel-size particles were observed. Distinct asperities and edges were also visible in subangular, bulky particles. Most of the platy particles had irregular shapes with very low sphericity and sharp edges. Figures 10(a) and 10(b) show the EAF(L) slag sand- and silt-size particles. The EAF(L) slag sand- and silt-size particles had subrounded to subangular shapes. Some very irregularly shaped platy particles were also observed. Most of the EAF(L) slag sand-size particles examined under SEM had extremely rough surface textures with platy, crystalline structures (see Figure 10). Some of the SEM micrographs of the EAF(L) slag sand-size particles indicated the presence of a porous structure.

10. Conclusions

The mineralogical and morphological properties of BOF and EAF(L) slag samples generated from two steel plants in

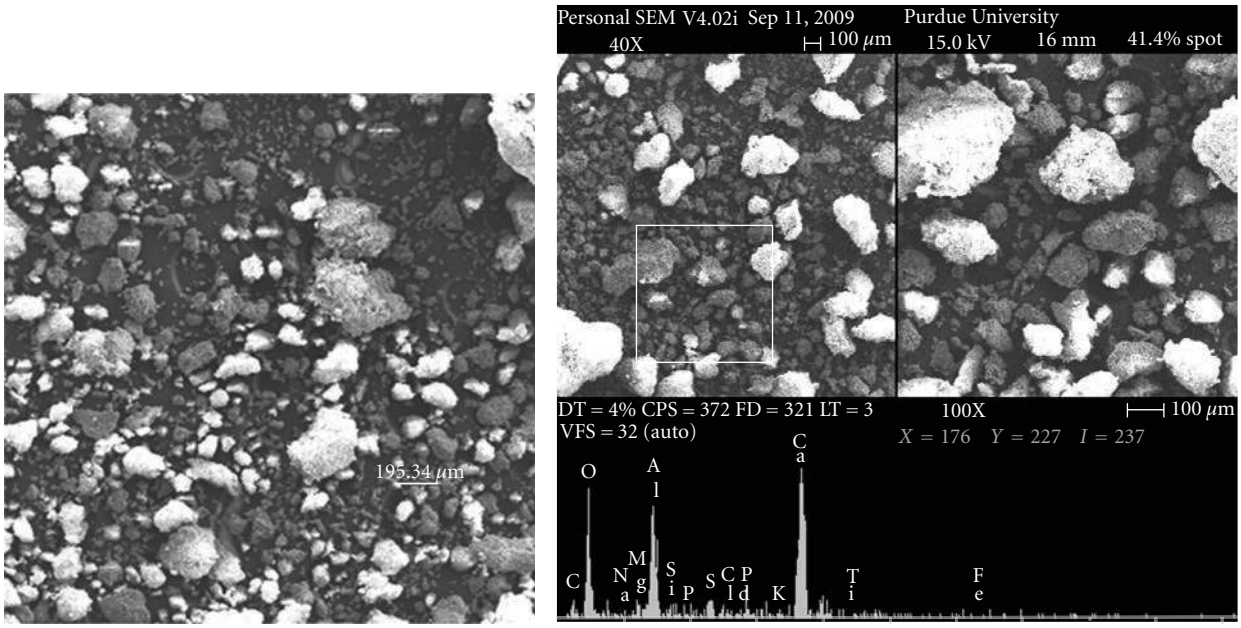

(a) (b)

Figure 10: SEM micrographs of EAF(L) slag. (a) sand- and silt-size particle shapes (magnification = 50X) and (b) particles with their elemental analysis.

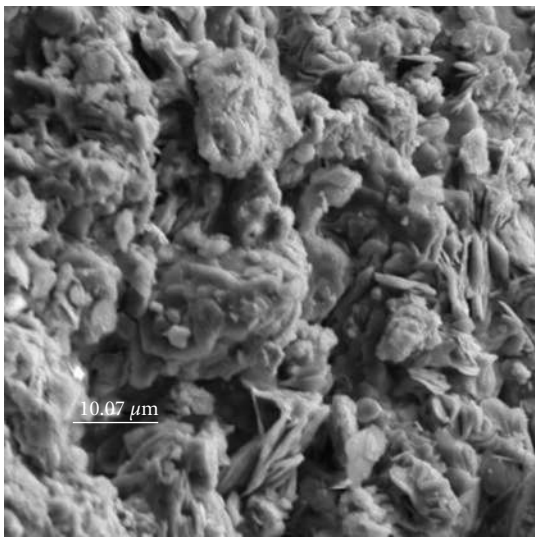

Figure 11: SEM micrograph showing the surface texture of a sand-size EAF slag particle (magnification = 1200X).

Indiana were investigated through XRD analyses and SEM studies. The following conclusions were reached.

(1) The main mineral phases identified in the BOF slag samples were Portlandite, srebrodol'skite, and merwinite.

(2) Most of the BOF slag gravel-size particles had a high sphericity and a solid structure. Sand- and silt-size BOF slag particles had subrounded to angular shapes and rough surface textures under SEM.

(3) The main mineral phases identified in the EAF(L) slag samples were portlandite, mayenite, and malenterite.

(4) Both bulky and platy gravel-size particles with very low sphericity and sharp edges were observed in the EAF(L) slag samples. Sand- and silt-size particles of EAF(L) slag samples showed subrounded to subangular shapes. SEM micrographs showed that the majority of the sand-size particles had extremely rough surface textures with distinct crystal structures.

(5) The morphological studies suggest that both the BOF and EAF(L) slag samples tested in this study have favorable frictional characteristics.

(6) The complex XRD patterns of the tested BOF and EAF(L) slag samples were a result of their chemical composition and the very slow cooling conditions applied during their processing. The XRD analyses of both the BOF and EAF(L) slag samples indicated the presence of free MgO and CaO. Since these compounds expand when hydrated, the volumetric instability of the tested steel slags needs to be assessed for their use in civil engineering applications.

Acknowledgments

This work was supported by the Joint Transportation Research Program administered by the Indiana Department of Transportation (INDOT) and Purdue University, Edw. C. Levy Co., and Multiserv Ltd., Harsco Corporation. The contents of this paper reflect the views of the writers, who are responsible for the facts and the accuracy of the data

presented herein. The contents neither necessarily reflect the official views or policies of the Indiana Department of Transportation, nor do the contents constitute a standard, specification or regulation. The writers are thankful to John Yzenas of Levy Co., and Nayyar Siddiki of INDOT for their support during this project.

References

[1] H. Schoenberger, "Final draft: best available techniques reference document on the production of iron and steel," Publications of EC: European Commission, Joint Research Centre, IPTS, European IPPC Bureau, 2001.

[2] Energy Manager Training (EMT), "Iron and steel process," July 2008, http://www.energymanagertraining.com/.

[3] D. Brandt and J. C. Warner, *Metallurgy Fundamentals*, Goodheart-Willcox, Tinley Park, Ill, USA, 3rd edition, 2005.

[4] American Iron and Steel Institute (AISI), "How Steel is Made," October 2011, http://www.steel.org/.

[5] S. Seetharaman, *Fundamentals of Metallurgy*, Woodhead Publishing and CRC Press, Boca Raton, Fla, USA, 2005.

[6] United Stated Geological Survey (USGS), "Slag-iron and steel," Annual Review, Mineral Industry Surveys, U.S. Geological Survey, Minerals Yearbook, Reston, Va, USA, 1993–2006.

[7] B. Das, S. Prakash, P. S. R. Reddy, and V. N. Misra, "An overview of utilization of slag and sludge from steel industries," *Resources, Conservation and Recycling*, vol. 50, no. 1, pp. 40–57, 2007.

[8] L. M. Juckes, "The volume stability of modern steelmaking slags," *Mineral Processing and Extractive Metallurgy*, vol. 112, no. 3, pp. 177–197, 2003.

[9] P. Y. Mahieux, J. E. Aubert, and G. Escadeillas, "Utilization of weathered basic oxygen furnace slag in the production of hydraulic road binders," *Construction and Building Materials*, vol. 23, no. 2, pp. 742–747, 2009.

[10] H. Y. Poh, G. S. Ghataora, and N. Ghazireh, "Soil stabilization using basic oxygen steel slag fines," *Journal of Materials in Civil Engineering*, vol. 18, no. 2, pp. 229–240, 2006.

[11] D. H. Shen, C. M. Wu, and J. C. Du, "Laboratory investigation of basic oxygen furnace slag for substitution of aggregate in porous asphalt mixture," *Construction and Building Materials*, vol. 23, no. 1, pp. 453–461, 2009.

[12] C. Shi, "Steel slag—its production, processing, characteristics, and cementitious properties," *Journal of Materials in Civil Engineering*, vol. 16, no. 3, pp. 230–236, 2004.

[13] M. Tossavainen, F. Engstrom, Q. Yang, N. Menad, M. L. Larsson, and B. Bjorkman, "Characteristics of steel slag under different cooling conditions," *Waste Management*, vol. 27, no. 10, pp. 1335–1344, 2007.

[14] J. Waligora, D. Bulteel, P. Degrugilliers, D. Damidot, J. L. Potdevin, and M. Measson, "Chemical and mineralogical characterizations of LD converter steel slags: a multi-analytical techniques approach," *Materials Characterization*, vol. 61, no. 1, pp. 39–48, 2010.

[15] W. Xuequan, Z. Hong, H. Xinkai, and L. Husen, "Study on steel slag and fly ash composite Portland cement," *Cement and Concrete Research*, vol. 29, no. 7, pp. 1103–1106, 1999.

[16] M. Barra, E. V. Ramonich, and M. A. Munoz, "Stabilization of soils with steel slag and cement for application in rural and low traffic roads," in *Proceedings of the Beneficial Use of Recycled Materials in Transportation Application*, pp. 423–432, RMCR University of Durham, Arlington, Va, November 2001.

[17] M. P. Luxán, R. Sotolongo, F. Dorrego, and E. Herrero, "Characteristics of the slags produced in the fusion of scrap steel by electric arc furnace," *Cement and Concrete Research*, vol. 30, no. 4, pp. 517–519, 2000.

[18] J. M. Manso, J. A. Polanco, M. Losañez, and J. J. González, "Durability of concrete made with EAF slag as aggregate," *Cement and Concrete Composites*, vol. 28, no. 6, pp. 528–534, 2006.

[19] P. E. Tsakiridis, G. D. Papadimitriou, S. Tsivilis, and C. Koroneos, "Utilization of steel slag for Portland cement clinker production," *Journal of Hazardous Materials*, vol. 152, no. 2, pp. 805–811, 2008.

[20] M. Nicolae, I. Vîlciu, and F. Zăman, "X-ray diffraction analysis of steel slag and blast furnace slag viewing their use for road construction," *UPB Scientific Bulletin Series B*, vol. 69, no. 2, pp. 99–108, 2007.

[21] G. R. Qian, D. D. Sun, J. H. Tay, and Z. Y. Lai, "Hydrothermal reaction and autoclave stability of Mg bearing RO phase in steel slag," *British Ceramic Transactions*, vol. 101, no. 4, pp. 159–164, 2002.

[22] J. Setién, D. Hernández, and J. J. González, "Characterization of ladle furnace basic slag for use as a construction material," *Construction and Building Materials*, vol. 23, no. 5, pp. 1788–1794, 2009.

[23] H. L. Robinson, "The utilization of blastfurnace and steel making slags as aggregates for construction," in *Proceedings of the 11th Extractive Industry Geology Conference*, pp. 327–330, The Geological Society of London, 2000, 36th forum on the Geology of Industrial Minerals, Industrial Minerals and Extractive Industry Geology.

[24] H. Shen, E. Forssberg, and U. Nordström, "Physicochemical and mineralogical properties of stainless steel slags oriented to metal recovery," *Resources, Conservation and Recycling*, vol. 40, no. 3, pp. 245–271, 2004.

[25] A. S. Reddy, R. K. Pradhan, and S. Chandra, "Utilization of Basic Oxygen Furnace (BOF) slag in the production of a hydraulic cement binder," *International Journal of Mineral Processing*, vol. 79, no. 2, pp. 98–105, 2006.

[26] A. Monaco and W. K. Wu, "The effect of cooling conditions on the characterization of steel slag," in *Proceedings of the International Symposium on Resource Conservation and Environmental Technologies in Metallurgical Industry*, pp. 107–116, Toronto, Canada, August 1994.

[27] C. Shi, "Characteristics and cementitious properties of ladle slag fines from steel production," *Cement and Concrete Research*, vol. 32, no. 3, pp. 459–462, 2002.

[28] J. M. Manso, M. Losañez, J. A. Polanco, and J. J. Gonzalez, "Ladle furnace slag in construction," *Journal of Materials in Civil Engineering*, vol. 17, no. 5, pp. 513–518, 2005.

[29] J. Geiseler, "Use of steelworks slag in Europe," *Waste Management*, vol. 16, no. 1–3, pp. 59–63, 1996.

[30] F. Wachsmuth, J. Geiseler, W. Fix, K. Koch, and K. Schwerdtfeger, "Contribution to the structure of BOF-slags and its influence on their volume stability," *Canadian Metallurgical Quarterly*, vol. 20, no. 3, pp. 279–284, 1981.

[31] G. Qian, D. D. Sun, J. H. Tay, Z. Lai, and G. Xu, "Autoclave properties of kirschsteinite-based steel slag," *Cement and Concrete Research*, vol. 32, no. 9, pp. 1377–1382, 2002.

[32] V. S. Ramachandran, P. J. Sereda, and R. F. Feldman, "Mechanism of hydration of calcium oxide," *Nature*, vol. 201, no. 4916, pp. 288–299, 1964.

[33] A. W. Kneller, J. Gupta, L. M. Borkowski, and D. Dollimore, "Determination of original free lime content of weathered iron and steel slags by thermogravimetric analysis," Transportation

Research Record 1434, Transportation Research Board, National Research Council, Washington, DC, USA, 1994.

[34] C. B. Crawford and K. N. Burn, "Building damage from expansive steel slag backfill," *Journal of the Soil Mechanics and Foundations Division*, vol. 95, no. 6, pp. 1325–1334, 1969.

[35] A. Verhasselt and F. Choquet, "Steel slags as unbound aggregate in road construction: problems and recommendations," in *Proceedings of the International Symposium on Unbound Aggregates in Roads*, pp. 204–211, London, UK, 1989.

[36] J. Geiseler, "Steel slag-generation, processing and utilization," in *Proceedings of the International Symposium on Resource Conservation and Environmental Technologies in Metallurgical Industry*, pp. 87–97, Toronto, Canada, August 1994.

[37] H. Motz and J. Geiseler, "Products of steel slags an opportunity to save natural resources," *Waste Management*, vol. 21, no. 3, pp. 285–293, 2001.

[38] I. A. Altun and I. Yilmaz, "Study on steel furnace slags with high MgO as additive in Portland cement," *Cement and Concrete Research*, vol. 32, no. 8, pp. 1247–1249, 2002.

[39] P. Chaurand, J. Rose, V. Briois et al., "Environmental impacts of steel slag reused in road construction: a crystallographic and molecular (XANES) approach," *Journal of Hazardous Materials*, vol. 139, no. 3, pp. 537–542, 2007.